Enhancing Log-Likelihood Ratios with Mutual Information on Three-Reader One-Track Detection in Staggered BPMR Systems

Natthakan Rueangnetr , Santi Koonkarnkhai , Piya Kovintavewat , Simon John Greaves , Chanon Warisarn *

Posted Date: 3 February 2025

doi: 10.20944/preprints202501.2382.v1

Keywords: bit-patterned magnetic recording (BPMR); log-likelihood ratio (LLR); multilayer perceptron (MLP); multitrack multi-head; mutual information

Article

Enhancing Log-Likelihood Ratios with Mutual Information on Three-Reader One-Track Detection in Staggered BPMR Systems

Natthakan Rueangnetr [1], Santi Koonkarnkhai [2], Piya Kovintavewat [2], Simon J. Greaves [3] and Chanon Warisarn [1,*]

[1] College of Advanced Manufacturing Innovation, King Mongkut's Institute of Technology Ladkrabang, Bangkok 10520, Thailand

[2] Faculty of Science and Technology, Nakhon Pathom Rajabhat University, Nakhon Pathom, 73000, Thailand

[3] Research Institute of Electrical Communication (RIEC), Tohoku University, Sendai, 980-8577, Japan

* Correspondence: chanon.wa@kmitl.ac.th; Tel.: +66 86-997-1001

Abstract: Because so much information is currently being shared online, there has been a sharp rise in the need for data storage devices over the past ten years. The main storage option is the hard disk drive (HDD), which is less expensive than some other types of data storage. Physical constraints, such as the superparamagnetic limit, are difficult to overcome using existing HDD technology. Consequently, bit-patterned magnetic recording (BPMR) has emerged as a potential solution, offering higher areal densities whilst maintaining thermal stability. Nevertheless, BPMR poses new challenges, such as inter-symbol interference and inter-track interference. Consequently, a number of approaches, such as staggered island layouts and array-reader magnetic recording, have been proposed to overcome these issues. However, this article proposes a three-reader one-track detection method to enhance data retrieval in a staggered BPMR system. Leveraging three-track reading for one-track detection, we obtain three readback signals that function as mutual data sequences. This substantially enhances the detection process in one-dimensional partial response maximum likelihood channels. Next, using these mutual data sequences, four novel techniques are presented to enhance bit-error rate (BER) performance and detection accuracy: hard-information flipping, maximum soft-information finding, bit-summation detection, and multilayer perceptron (MLP). This study shows that these proposed techniques can provide better BER performance compared with conventional methods and that the MLP is the most effective technique in enhancing system performance.

Keywords: bit-patterned magnetic recording (BPMR); log-likelihood ratio (LLR); multilayer perceptron (MLP); multitrack multi-head; mutual information

1. Introduction

With the ongoing, rapid increase in the amount of information generated by consumers, the capacity of data storage devices must also increase to meet the ever-growing demand for storage. Hard disk drives (HDDs) are currently the main devices used to meet this need. The HDD technology used today, known as perpendicular magnetic recording (PMR), is having trouble overcoming several technical and physical limitations. The growing areal density (AD) of PMR is restricted because of the superparamagnetic limit [1], where thermal energy can cause the magnetization of media grains to become unstable and randomly change direction [2]. Hence, other magnetic recording methods are needed to extend the AD of HDDs above 1 Tera-bit per square inch (Tb/in^2). As a result, some researchers have suggested using different magnetic recording methods to increase the AD of HDDs. Bit-patterned magnetic recording (BPMR) [3], [4] is one of the most intriguing suggested recording methods, since it has the potential to reach an AD of up to 4.0 Tb/in^2 [1].

 doi:10.20944/preprints202501.2382.v1

In contrast to PMR, BPMR can reduce transition noise in granular media by storing each data bit on a separate magnetic island segregated by non-magnetic material [5]. To increase AD in BPMR, it is necessary to decrease the separation between magnetic islands. Typically, a reader is used to detect the magnetization of the magnetic islands. In the reading data process, the reader covers multiple islands in both the down-track and cross-track directions as it is usually wider than the track width [6].

In this scenario, the readback signal processing is challenging because of inter-symbol interference (ISI) and inter-track interference (ITI), also known as two-dimensional (2D) interference [7–9]. The severity of the 2D interference is dependent upon the operating AD, i.e., the higher the AD, the more severe the 2D interference. Another factor that may affect the BPMR system performance is media noise arising from imperfections in fabricating the recording medium, and this can have a major impact on the system performance [8], [9]. In general, the primary sources of media noise stem from variations in the size and position of the magnetic islands. As a result, introducing a signal processing system that can handle 2D interference and media noise is crucial to realizing higher ADs. Numerous solutions have been proposed in the literature to tackle 2D interference and media noise during signal processing in BPMR systems. Changing the medium configuration is one such technique.

Notably, research in [10–12] suggested that utilizing staggered island arrays, instead of rectangular island arrays, can enhance the bit-error rate (BER) performance at the same AD. Staggered Island arrays have been proven to be effective in mitigating the impact of ITI caused by the presence of adjacent tracks. Moreover, an array-reader magnetic recording (ARMR) is a signal processing technique that has been implemented in BPMR systems [13–15]. ARMR involves the simultaneous processing of signals from multiple readers, which allows for robust information recovery in ultrahigh AD BPMR systems when compared with a single-reader system [16]. The multiple readers yield multiple readback signals that correlate with the interference, thus improving the detection process. Furthermore, dual-reader ARMR has been utilized to evaluate the skew-induced variation in cross-track separation for increasing the recording performance [17].

The one-dimensional (1D) partial-response maximum-likelihood (PRML) technique is an essential and comprehensive approach that characterizes the signal's partial response, adapts to changing signal conditions through adaptive equalization, utilizes the soft-output Viterbi algorithm (SOVA) for efficient detection, and can incorporate error correction coding to enhance data reliability. It is an essential technique that plays a vital role in ensuring accurate and reliable data retrieval in magnetic recording. In addition, improving the soft information or log-likelihood ratio (LLR) generated from the SOVA detector is also proposed to enhance the overall system performance. For instance, the encoding criteria of a modulation encoder are utilized to improve the LLRs before sending them to the decoders [18,19]. Specifically, the encoding condition is used as the criterion for flipping the obtained LLRs: as a result, the LLRs can be significantly enhanced, improving system performance.

Moreover, recent advances in deep neural networks (DNNs) have also revolutionized the approach to signal processing in magnetic recording. The proposed DNN-based detectors in [20–22] can accurately produce soft-output information, which significantly simplifies turbo decoding. The combination of the DNN-based predictor with conventional detection reveals that it can improve detection accuracy, as suggested in [23,24]. Furthermore, in [25], DNNs, such as long-short-term memory (LSTM) networks, and supervised learning were also utilized to improve LLR reliability, resulting in better BER performance. Hence, the use of DNNs significantly improves LLR reliability and is a suitable solution for signal processing in ultra-high-density BPMR systems.

In this study, since the reliabilities of the soft information generated by the 1D SOVA detectors were affected by defects in the readback signals, these reliabilities must be carefully addressed. Generally, these defects are primarily caused by 2D interference and media noise. To improve the detection process, we propose enhancing the soft information output produced by the 1D SOVA detector before making a final decision. This can be achieved through four proposed techniques, namely, hard-information flipping (HIF), maximum soft-information (MSI) finding, bit-summation

 doi:10.20944/preprints202501.2382.v1

detection (BSD), and multilayer perceptron (MLP). These proposed techniques can operate together with the staggered bit island arrangement using an array reader. The study shows that these proposed methods outperform the conventional methods in terms of BER and frame-error rate (FER) performances. Additionally, our findings also show that the proposed techniques were effective against media noise, which consisted of position and size variations. Furthermore, an MLP is the most effective approach to enhance system performance.

The remainder of this paper is organized as follows. Section 2 describes the staggered BPMR channel model. Section 3 explains the proposed techniques. Section 4 reports the performance evaluation, and Section 5 concludes this work.

2. BPMR Channel Model

This article presents a staggered island BPMR medium using a three-reader one-track detection scheme, as illustrated in Figure 1. The readback signal from the desired track experiences ITI from both upper and lower adjacent tracks, while these adjacent tracks similarly experience ITI from the desired track. Thus, we expect that some information from the desired track is embedded within the readback signals of the adjacent tracks, creating a form of mutual information. A key contribution is to utilize this mutual information to improve the quality of the estimated user bits, thereby enhancing overall system performance.

Figure 2 depicts the cross-sectional view of the head-medium geometry in the staggered BPMR system used in this study. The soft-magnetic underlayer (SUL) thickness was 300 nanometers (nm), the non-magnetic interlayer (IL) thickness was 15 nm, the recording layer (RL) thickness was 10 nm, and the head-medium spacing (HMS) was 5 nm, which was the distance between the air-bearing surface (ABS) of the read/write head and the top surface of the RL.

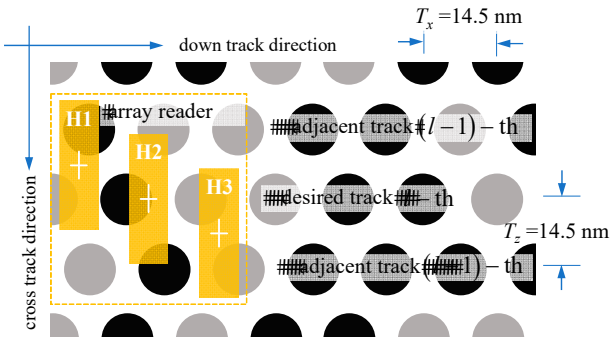

Figure 1. Staggered bit-patterned recording medium and three-reader array at an AD of 3.0 Tb/in².

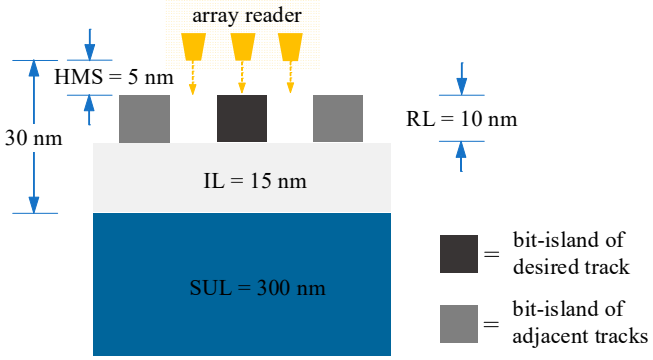

Figure 2. Staggered bit-patterned recording medium and three-reader array at an AD of 3.0 Tb/in².

To model the staggered BPMR medium, as shown in Figure 3, we arranged a series of circular magnetic islands, each with a diameter of 10 nm, in a staggered pattern on a non-magnetic surface,

 doi:10.20944/preprints202501.2382.v1

represented by the white region. The gray and black islands indicate magnetization directions of "down" (−1) and "up" (+1), respectively. Figure 3 shows the center reader among three readers packed in an array reader, with its readhead sensitivity focused on reading data from the desired track. The readhead sensitivity extends to adjacent tracks, which causes the ITI effect. The AD was determined by the bit period (T_x) and track pitch (Tz). For example, the AD equals 3.0 Tb/in² when $T_x = T_z = 14.5$ nm.

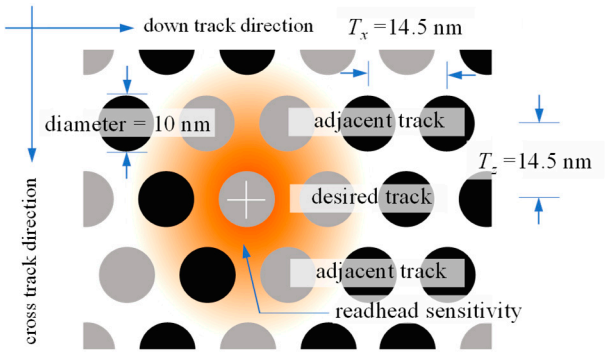

Figure 3. Configuration of the staggered BPMR array at an AD of 3.0 Tb/in², showing the extent of the read head sensitivity response.

Additionally, bit island size and position fluctuations were incorporated as sources of media noise to provide a more realistic BPMR channel model. Specifically, the size fluctuation was defined as

$$\text{size fluctuation} = \frac{\sigma_d}{d}, \tag{1}$$

where d is the ideal diameter of the bit island, and σ_d is the variance of the bit island diameter (a Gaussian distribution). Moreover, the position fluctuation was defined as

$$\text{position fluctuation} = \frac{\sigma_{T_x}}{T_x}, \tag{2}$$

where T_x is the bit period, and σ_{Tx} is the variance of the distance between the centers of the bit islands (a Gaussian distribution). Note that the size and position fluctuations in this study were independent and identically distributed (*i.i.d*) random variables. This paper considers the staggered medium for three-reader one-track detection depicted in Figure 1, in conjunction with the channel model shown in Figure 4. A 4096-bit user sequence $u_{k,l} \in \{\pm 1\}$, where the bits were defined as *i.i.d* random variables, commonly used in various studies of magnetic recording channels, was recorded onto the medium. A perfect writing process was assumed, in which the magnetization of the bit islands was always the same as the intended bit sequence.

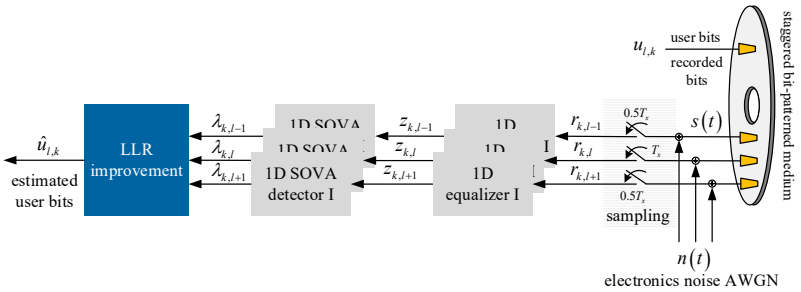

Figure 4. Block diagram of the three-reader one-track detection BPMR channel with the proposed improvement techniques.

 doi:10.20944/preprints202501.2382.v1

During a reading process, an array of three read heads simultaneously detects these three data tracks (or uses a single read head to sequentially detect these tracks with the help of buffer memory), as illustrated in Figure 1. As for our read head arrangement, the middle reader (H2) was positioned at the center of track l, referred to as the desired track. The upper reader (H1) was placed between tracks (l−1) and l, while the lower reader (H3) was placed between tracks l and (l+1). To utilize the mutual information from the upper and lower tracks, H1 and H3 were moved toward the desired track by half the track pitch. This helped increase the correlation of this mutual information, thus enabling us to improve the BER performance of the desired track using our proposed methods. It is important to highlight that track misregistration is a concern during the reading process; however, prediction and correction techniques using the array reader may be adopted to cope with this unavoidable situation as proposed in [26–28].

To obtain the readback signal, $s(x,y)$, as a function of x and y coordinates (in nanometers), the magnetization of each bit island in the recording medium, $m(x,y)\in\{\pm1\}$, was convolved with the reader sensitivity function, $h(x,y)$, [29,30]. Therefore, the readback signal $s(x,y)$ can be expressed as

$$s(x,y) = \iint m(\xi,\eta)h(x-\xi,y-\eta)d\xi d\eta. \tag{3}$$

Considering the reading process in the time domain, the continuous-time readback signal, $r(t)$, can be obtained by setting $s(t) = s(t,i)$, where i is the center of the reader sensitivity function in the cross-track direction. Thus, the continuous-time readback signal, $r(t)$, can be obtained by

$$r(t) = s(t)+n(t), \tag{4}$$

where $n(t)$ is additive white Gaussian noise, with the power spectral density being flat across the entire sampling bandwidth. Here, $n(t)$ can be calculated from

$$n(t) = \sigma\cdot Z, \tag{5}$$

where

$$\sigma = A\Big/\sqrt{10^{\mathrm{SNR}/10}} \tag{6}$$

and $Z \sim N(0,1)$ is a random variable that follows the standard normal distribution with zero mean and a standard deviation/variance of 1, $A = 1$ is the peak amplitude of the normalized readback signal for an isolated transition, and SNR is the signal-to-noise ratio in decibels (dBs).

Assuming perfect synchronization, the discrete-time readback sequence for the (l−1)-th and (l+1)-th tracks, $r_{k,l-1}$ and $r_{k,l+1}$, was obtained by over-sampling $r_{l-1}(t)$ and $r_{l+1}(t)$ at time $t = 0.5kT_x$. However, the data sequence of the l-th track, $r_{k,l}$, was obtained by sampling the readback signal $r_l(t)$ at time $t = kT_x$. Therefore, three data sequences or three mutual data sequences were produced. Next, the three readback signal sequences $\{r_{k,l-1}, r_{k,l}, r_{k,l+1}\}$ were fed to the equalizers to output the equalized data sequences $\{z_{k,l-1}, z_{k,l}, z_{k,l+1}\}$ according to their target responses. The equalized data were then sent to the SOVA detectors to estimate the most likely recording bit sequences in the form of soft-output information, or LLR, of each track $\{\lambda_{k,l-1}, \lambda_{k,l}, \lambda_{k,l+1}\}$. Then, to improve the reliability of LLR sequences produced from such detectors before making a final decision, four proposed LLR improvement techniques based on mutual data were employed, namely, HIF, MSI, BSD, and MLP. Finally, the estimated user bits were compared with the actual user bits to calculate the BER.

3. Proposed Methods

This section explains four data detection techniques that rely on mutual data to improve the LLR during the detection process to enhance the system's performance. Before doing so, we first examine the distributions of readback signals obtained from staggered BPMR media, as shown in Figure 5.

Three readback signals were obtained from three read-heads (H1, H2, and H3), and the distribution of the sample amplitudes of each readback signal is depicted in Figure 5 without electronic noise. The dots denote the data obtained by sampling the readback signal. The red dots represent the samples obtained from the desired l-th track, whereas the black dots represent the

 doi:10.20944/preprints202501.2382.v1

samples from the (l-1)-th and (l+1)-th tracks. As a result, we note that the sample amplitude distribution retrieved from the desired track using H2 was more explicit than that from H1 and H3. This implies that the signal carrying the desired data from H2 was significantly stronger than that from H1 and H3.

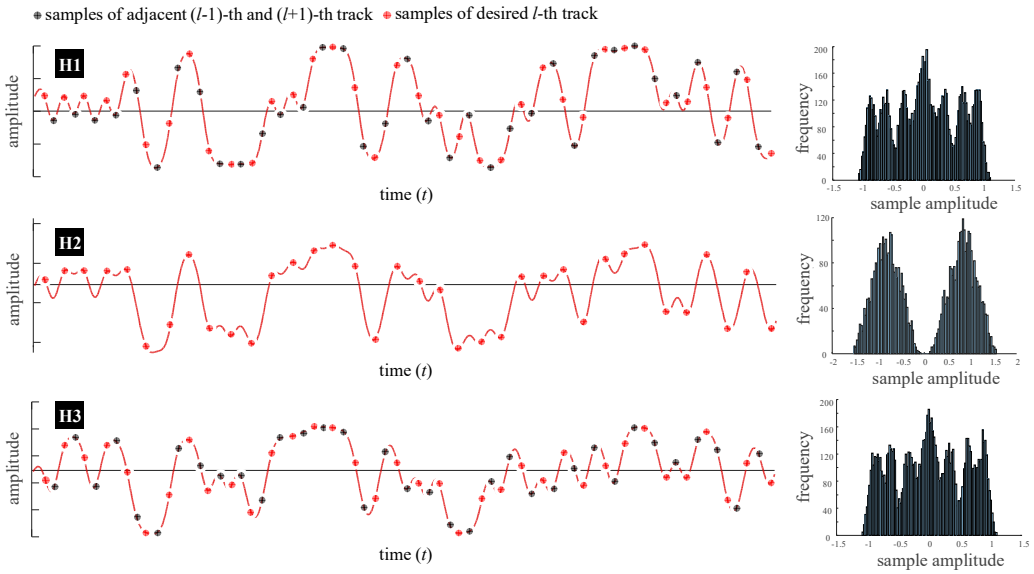

Figure 5. Readback signal waveforms from a staggered medium at AD = 3.0 Tb/in².

It is assumed that the data samples produced from H1 and H3 at the k-th bit can help enhance the quality and reliability of the k-th bit obtained from H2, which is the desired readback signal. After SOVA detection, three mutual samples of soft information representing one recorded bit are obtained. These data samples are referred to as mutual data information. To improve the LLR in the detection process, we propose four techniques that utilize mutual data information, which are described as follows.

3.1. Hard Information Flipping (HIF)

We first examine three mutual data bits (hard information) produced by 1D SOVA detectors, represented as a 3×1 column vector, as shown in Figure 6(a). These bits were produced from the LLRs generated by SOVA detectors through a threshold detector. The first and third rows correspond to the data from H1 and H3, respectively, while the second row is from H2. Practically, these three estimated bits should have the same sign as the recorded bit being detected.

Therefore, disagreement among the signs indicates the presence of errors, and to maximize accuracy, a simple scheme is to select the most common sign among the three. For instance, in the first and last columns of Figure 6(a), when all three bits are '+1s' or '-1s', the estimated recorded bits will be '+1' and '-1', respectively, as depicted in the first and last columns of Figure 6(b). Referring to the second column in Figure 6(a), there are two '+1s' and one '-1'. In this case, the most common sign, '+1', is selected as the estimated recorded bit. Similarly, in the fifth column, there are two '-1s' and one '+1'. Therefore, the estimated recorded bit for this column is '-1', as depicted in Figure 6(b).

3.2. Maximum Soft Information (MSI) Finding

For the MSI finding technique, we start by considering three mutual data in the form of three soft-information values or LLRs produced by 1D SOVA detectors in a 3×1 column vector, i.e., $[\lambda_{k,-1}, \lambda_{k,0}, \lambda_{k,1}]^T$, similar to HIF. Here, $[\cdot]^T$ is a transpose operator. To better understand the MSI process, we can refer to the flowchart displayed in Figure 7, which can be described as follows.

Preprints.org (www.preprints.org) | NOT PEER-REVIEWED | Posted: 3 February 2025 doi:10.20944/preprints202501.2382.v1

Step 1: Given a 3×1 vector $\boldsymbol{\lambda} = [\lambda_{k,-1}, \lambda_{k,0}, \lambda_{k,1}]^T$, we check if the signs are either $[+, +, +]^T$ or $[-, -, -]^T$, the estimated user bit, $\hat{u}_{k,0}$, will be determined based on that particular symbol.

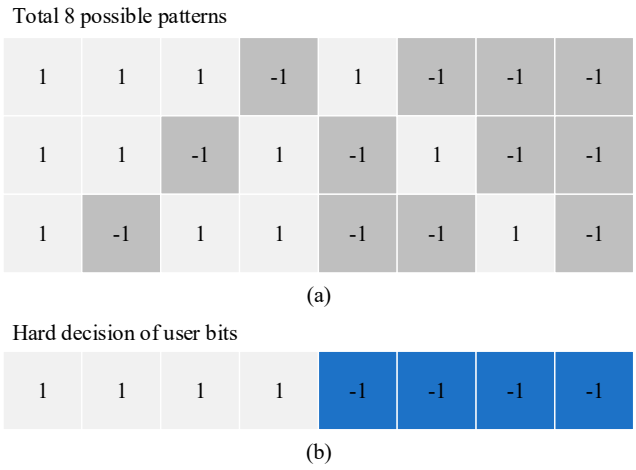

Figure 6. Example of HIF technique operation.

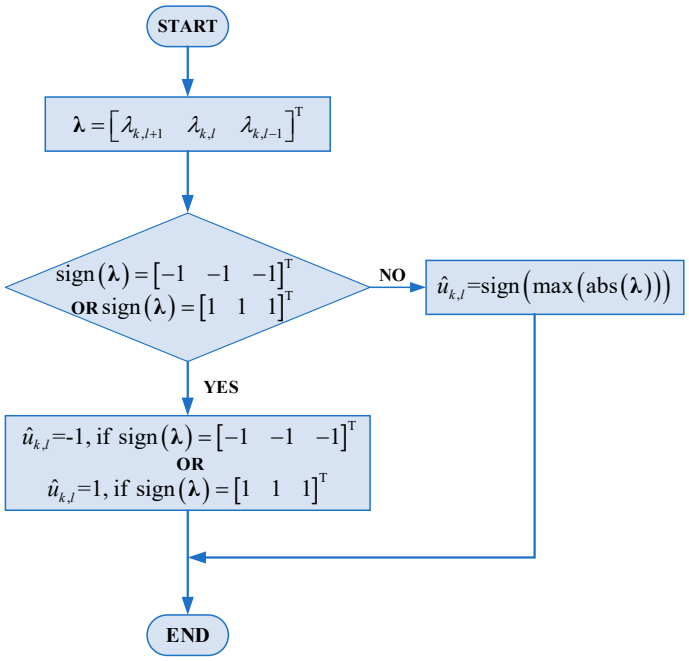

Figure 7. A flowchart explaining the MSI technique.

Step 2: If the signs of all elements in $\boldsymbol{\lambda}$ are not identical, we choose the element that has a maximum absolute value. Then, the sign of the chosen element will determine the estimated user bit.

Figure 8 illustrates an example of how the MSI technique operates. The LLRs associated with the three tracks are produced from the 1D SOVA detectors at SNR = 8 dB as shown in Figure 8(a). For instance, all elements in the first and second columns have the same sign, and the estimated user bit is determined accordingly. However, the signs of the elements in the fourth column are not identical, with a maximum absolute value of -30.47. In this case, the estimated user bit of the fourth column will be '-1' as shown in Figure 8(b). Similarly, in the fifth column, the highest absolute value is 13.72, and the estimated user bit will be '+1.'

 doi:10.20944/preprints202501.2382.v1

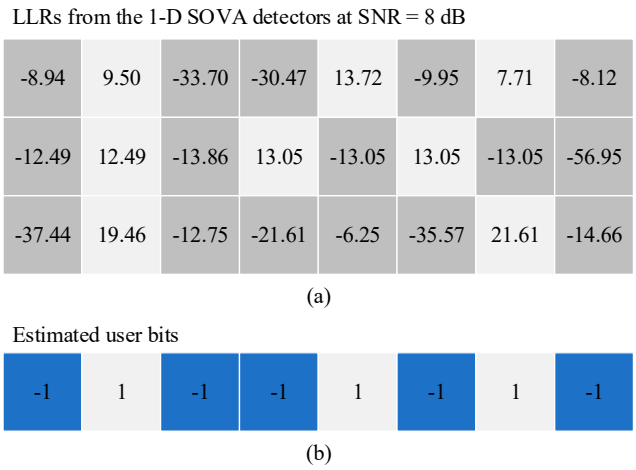

Figure 8. Example of MSI technique operation.

3.3. Bit-Summation Detection (BSD)

We begin with the 3×1 LLR vector obtained from the 1D SOVA detectors $[\lambda_{k,-1}, \lambda_{k,0}, \lambda_{k,1}]^T$. As mentioned earlier, all three readback signals convey some information about the k-th user bit on the desired track, $u_{k,0}$. In the BSD technique, we propose to improve the LLR of $u_{k,0}$ by using

$$\sigma = A\Big/\sqrt{10^{\mathrm{SNR}/10}} \tag{7}$$

where the derivation of (7) is given in Appendix A. Then, the improved LLR, $\hat{LLR}$, in eq. (7) is sent to the threshold detector to determine the estimated user bits, $\hat{u}_{k,0}$.

An example of how the BSD technique operates is demonstrated in Figure 9. First, the LLRs produced from the 1D SOVA detectors are arranged in a 3×1 column vector, i.e., $[\lambda_{k,-1}, \lambda_{k,0}, \lambda_{k,1}]^T$, as in Figure 9(a). Then, the elements in each column are summed according to (7) to obtain the improved LLRs as shown in Figure 9(b). Finally, the estimated user bits are obtained by passing the improved LLRs through a threshold detector, giving the results shown in Figure 9(c).

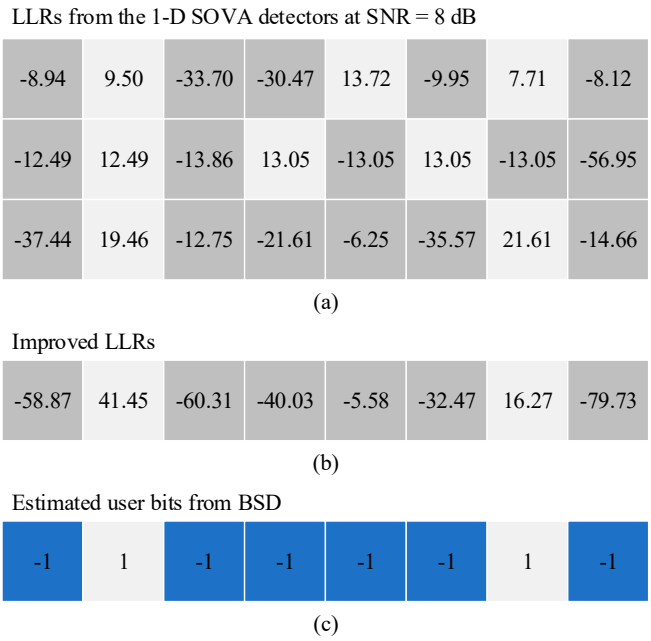

Figure 9. Example of BSD technique operation.

Preprints.org (www.preprints.org) | NOT PEER-REVIEWED | Posted: 3 February 2025 doi:10.20944/preprints202501.2382.v1

3.4. Multilayer Perceptron (MLP)

The MLP is a popular choice for signal processing in a magnetic recording system because it has enough power to learn the characteristics of noise and interference within a reasonable amount of computational complexity. MLP is a type of feedforward neural network, where all nodes are fully connected, and a nonlinear activation function is used in every node.

Figure 10 illustrates the proposed MLP architecture. The idea is to employ one single network to process all LLR mutual data sequences obtained from the 1D SOVA detectors. As depicted in Figure 10, the MLP takes the LLRs $[\lambda_{k,-1}, \lambda_{k,0}, \lambda_{k,1}]^T$ obtained from the 1D SOVA detectors as inputs to improve prediction robustness [20], and generates the corresponding user bit sequence as an output. This MLP consists of neurons arranged in stacked, fully connected layers. Each neuron calculates its output and passes the data to the next layer. Additionally, this MLP has seven layers, i.e., one input layer, five fully connected hidden layers, and one output layer.

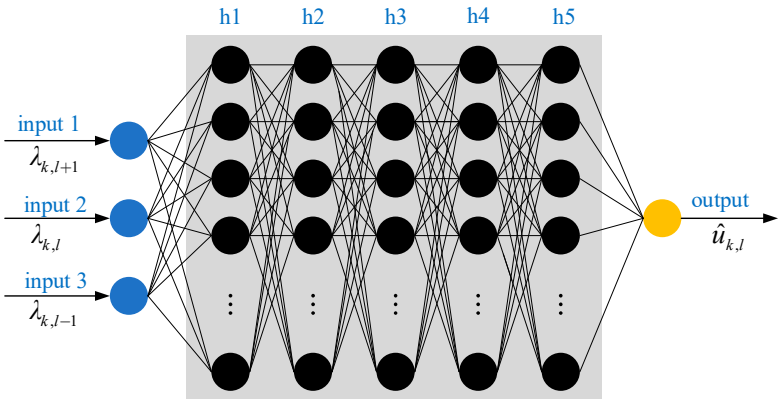

Figure 10. Structure of MLP-based soft-information flipper.

We used a sliding window approach on the LLR sequences obtained from the 1D SOVA detectors. Specifically, the data was processed in blocks, and the block window slid over time to observe successive data blocks, hence the term "sliding window." By carefully selecting the block size and sliding step size, the MLP can be used effectively to provide good prediction. Before feeding a sequence into the MLP, the sequences must be converted into vectors to satisfy the input layer condition, which processes data in vector form only.

Let $\boldsymbol{\lambda} = [\lambda_{k,-1}, \lambda_{k,0}, \lambda_{k,1}]$ be the input vector, which was fed to 5 fully connected hidden layers with 100 neurons in each layer. For each neuron, a linear combination of all input entries was computed using a weight vector and a bias value specific to that neuron. Specifically, given an input vector, $\boldsymbol{\lambda}$, the output vector, $\hat{\mathbf{u}}$, obtained from the linear combination can be written as

$$\hat{\mathbf{u}} = \mathbf{W}\lambda + \mathbf{b}, \tag{8}$$

where $\mathbf{W}$ is an $n_z \times n_x$ weight matrix, $\mathbf{b}$ is an $n_z \times 1$ bias vector, n_z is the number of neurons, and n_x is the number of elements in the input vector.

Then, a nonlinear activation function was applied to the vector, $\hat{\mathbf{u}}$, yielding the final output vector of the fully-connected layer. In this paper, we used the rectified linear function (ReLU) as the nonlinear activation function since it provided computational efficiency and could alleviate the vanishing gradient problem, where the ReLU output can be written as

$$\mathbf{y} = \mathrm{ReLU}(\hat{\mathbf{u}}), \tag{9}$$

where $y_k = \max(0, u_k)$. For the output layer, this network solved the binary classification problem by assigning each input vector sample a class label of either –1 or +1, corresponding to the user bit. The softmax function was used for this binary classification task, whose output was given by

 doi:10.20944/preprints202501.2382.v1

$$\mathbf{y} = \sigma(\lambda), \ : y_n = \frac{e^{\lambda_n}}{\sum_{j=1}^{K} e^{\lambda_j}}, n = 1, ..., K. \tag{10}$$

where $\boldsymbol{\lambda}$ and $\mathbf{y}$ are the input and the output vectors of the softmax function, respectively.

Because our MLP solved a binary classification problem, the network output was the probability of its respective class label. Hence, this probability can be converted into soft information, or LLR, according to

$$\lambda_{k,l} = \ln\left(\frac{p(a_{k,l} = +1)}{p(a_{k,l} = -1)}\right) = \ln\left(\frac{y_2}{y_1}\right), \tag{11}$$

where y_2 and y_1 are the probability of network prediction, labeled as class +1 and –1, respectively, and $p(a_{k,l} = +1) = 1 - p(a_{k,l} = -1)$. The LLR value obtained from this procedure was concatenated for each time step, resulting in the LLR sequence.

During the training process, we explored different training strategies for the proposed MLP. The MLP input consisted of three LLRs obtained from 1D SOVA detectors, whereas the MLP output represented the hard information corresponding to the user bit. In this study, the input dataset ($\boldsymbol{\lambda}$) was a 3×3,000 matrix, and the output dataset ($\hat{\mathbf{u}}$) was a 1×3,000 matrix. To generate the input dataset, we ignored all media noise, and the SNR was randomly varied from 1 to 20 dB. A learning rate of 0.001 was employed, and the model was trained over 50 epochs using the Adam optimizer. This resulted in an optimized MLP model that was able to directly map three LLR sequences to one user data sequence, as shown in Figure. 10.

4. Simulation Results

In this study, six systems were evaluated: System I (1D conventional and 2D conventional systems, without LLR enhancement), System II (HIF), System III (MSI), System IV (BSD), and System V (MLP). Our evaluation was based on an AD of 3.0 Tb/in^2. Figure 11 illustrates the LLR distributions of the five systems under the same conditions with SNR = 12 dB and the media noise was neglected. In the Figureure, the blue dots represent correct LLRs, while the red cross symbols denote erroneous LLRs. The x-axis represents the bit number, set at 50,000 bits, whereas the y-axis displays the LLR values generated from the 1D SOVA detectors, except for the 2D conventional system in the LLR values generated by the 2D SOVA detectors [31]. Subfigureures (a) to (f) correspond to Systems I to V, respectively. Upon observing Figure 11, it is evident that the conventional system exhibited higher erroneous LLRs than the other systems. Conversely, System V demonstrated superior LLR performance, with only 94 erroneous bits, as shown in Figure 11(f).

Next, we explored the BER performance of the proposed systems without position and size fluctuations as shown in Figure 12, where each BER point was computed using as many data sectors as needed to collect 500 error bits. The proposed systems exhibited significant performance improvements when compared to the 1D and 2D conventional systems. In this process, a 2D equalization combined with 2D detection, utilizing a 2D minimum mean square error (MMSE) equalizer [7] and a 2D SOVA detector [31], is applied to process the retrieved readback signals. The size of the 2D MMSE equalizer coefficient is 3×11 taps and the size of the target coefficient of the 2D SOVA detector is 3×3 taps, which means the side track information is used to jointly design the detection process.

Three retrieved readback signals are also read using three readers as similarly used in 1D processing. Specifically, Systems II, III, IV, and V achieved gains of 3.2, 4.0, 4.6, and 5.1 dB, respectively, over the 1D conventional system at BER = 10^{-5}. Moreover, the proposed MLP technique can approximately gain 2.0 dB over the 2D conventional system. The 2D conventional system offers better BER performance compared to the 1D conventional system because it can deal with the effect of ITI. Additionally, it also outperforms the proposed techniques—HIF, MSI, and BSD—at lower SNRs. However, at higher SNRs, the proposed techniques demonstrate improved performance,

 doi:10.20944/preprints202501.2382.v1

indicating their effectiveness in managing the effects of ITI. Notably, the proposed MLP technique consistently achieves the best performance across all SNR levels.

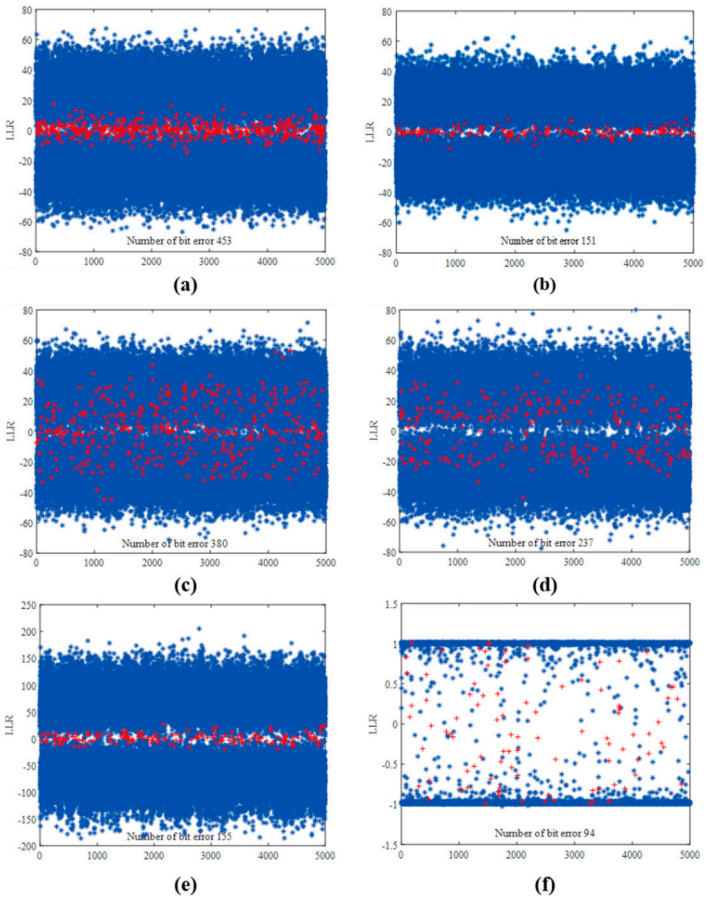

Figure 11. LLR distributions of (a) System I: 1D conventional, (b), System I: 2D conventional, (c) System II: HIF, (d) System III (MSI), (e) System IV: BSD, and (f) System V: MLP, for SNR = 12 dB and AD = 3.0 Tb/in^2.

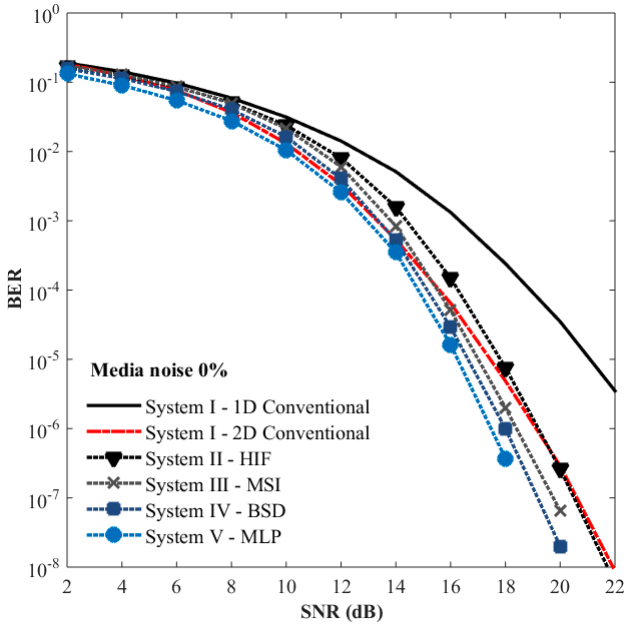

Figure 12. BER performance of the proposed systems without position and size fluctuation.

 doi:10.20944/preprints202501.2382.v1

After introducing 5% media noise (position and size fluctuations), the superiority of the proposed systems over the conventional system remained evident. Specifically, Systems II, III, IV, and V achieved gains of 2.7, 3.2, 4.1, and 5.3 dB, respectively, at BER = 10^{-5} over the 1D conventional system, as depicted in Figure 13. Additionally, it is clear that 2D processing can offer better performance compared to the 1D processing technique, which means that the ITI effect can be effectively managed by considering the information from its side tracks through 2D signal processing. However, the proposed MLP technique still provide better BER performance compared with the 2D conventional system.

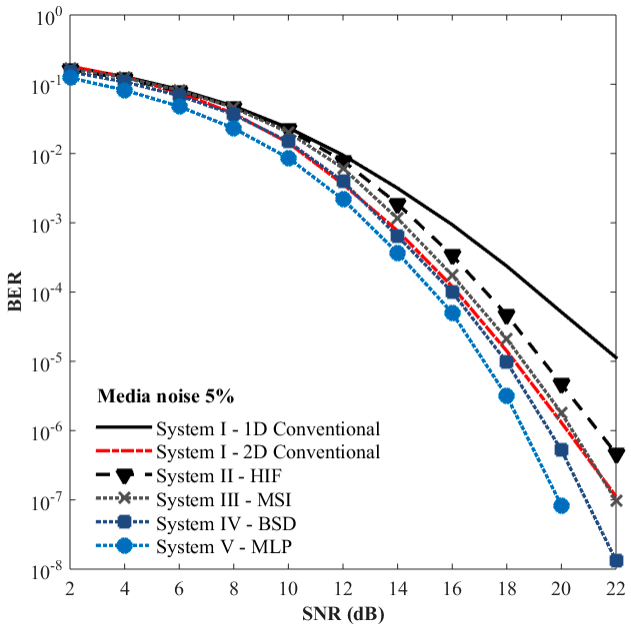

Figure 13. BER performance of the proposed systems with position and size fluctuations at 5%.

Furthermore, we also evaluated the proposed systems under severe media noise conditions (i.e., 10% media noise), as illustrated in Figure 14. The results reveal that the severity of media noise affects all systems, significantly degrading their BER performance. However, all proposed systems maintained superior BER performance compared to the 1D conventional system. Specifically, at BER = 10^{-4}, Systems II, III, IV, and V achieved gains of 2.4, 3.9, 4.5, and 5.0 dB, respectively, over the 1D conventional system. The 2D conventional system gains around 2.5 dB over the 1D conventional system at BER = 10^{-4}, which means that it is not only deal with ITI effect but also cope with the media noise effectively. However, proposed MLP technique provides the best BER performance. This demonstrates the robustness of our proposed systems even under severe media noise conditions.

We also analyzed the system performance using frame error rate (FER) versus SNR at an AD of 3.0 Tb/in^2 without media noise as shown in Figure 15. Each FER point was calculated using as many 4096-bit sectors as needed to collect 1000 error frames or sectors. The results show that our proposed systems outperformed the 1D conventional system. In particular, at FER = 10^{-3}, System V can approximately provide gains of 3.1, 2.0, and 1.2 dB over Systems II, III, and IV, respectively, while the 1D conventional system cannot achieve FER of 10^{-3} with an SNR of 20 dB. Among all proposed systems, the MLP-based approach demonstrated the highest performance improvement. Based on these results, all the proposed systems outperformed the 1D conventional system. Notably, System V, utilizing the MLP algorithm, showed superior performance and provide a better performance compared with the 2D conventional system. This might be because the MLP demonstrated an ability to understand the characteristics of the readback signals. System IV, closely followed, leveraging the LLR for maximum data reliability detection. In this technique, a high LLR signified a high reliability of the data bit, and the BSD technique, which sums LLR mutual data, further enhanced the reliability

 doi:10.20944/preprints202501.2382.v1

of detected bits. It is important to note that, with the MLP's capability, it could directly process the readback signals without needing to be cascaded after the SOVA detector. It may use the readback signals for MLP training and learning. However, since the other three proposed systems were specifically designed to enhance LLRs obtained from the SOVA detectors, comparing their performance with that of the cascaded MLP approach provides valuable insights for this study. Additionally, System II aimed to maximize LLR mutual data, resulting in higher reliability of data detection. By emphasizing the summation of LLR, the detection of incorrect bits became highly reliable. In contrast, System III prioritized the probability of flipping incorrect data bits to correct ones by considering the maximum probability of LLR mutual data. In summary, the MLP algorithm in System V, the LLR-based techniques in Systems II and IV, and the probability considerations in System III collectively contributed to the enhanced performance of the proposed systems over the conventional system.

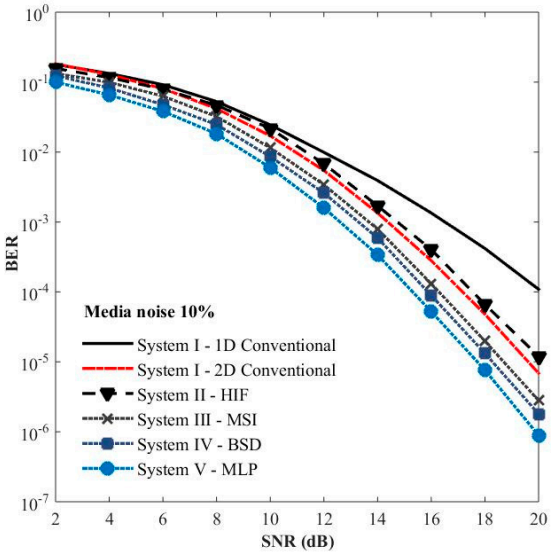

Figure 14. BER performance of the proposed systems with position and size fluctuations at 10%.

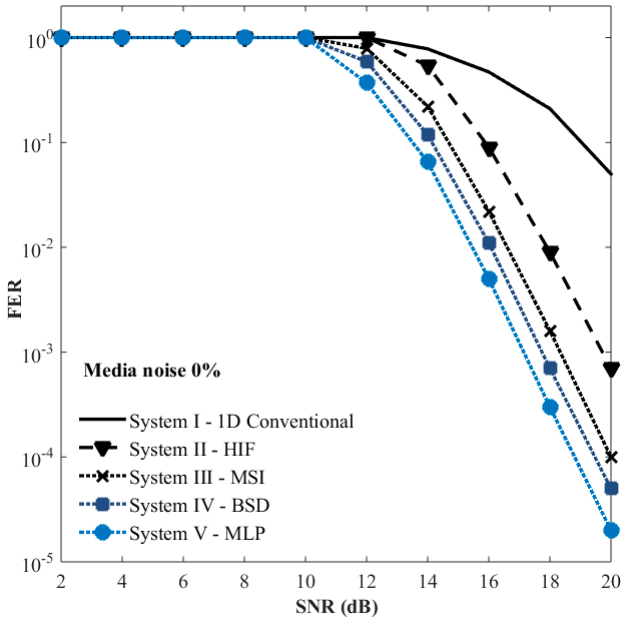

Figure 15. FER performance of the proposed systems without position and size fluctuations.

 doi:10.20944/preprints202501.2382.v1

5. Conclusion

In ultra-high-density bit-patterned magnetic recording (BPMR) systems, two-dimensional (2D) interference significantly impacts the overall system performance. To mitigate this issue, we proposed the use of an array-reader magnetic recording (ARMR) in a staggered BPMR system for detecting a single data track. An ARMR generates multi-readback signals to detect mutual data. We then leveraged this mutual data during the detection process by employing four different techniques to enhance the log-likelihood ratio (LLR) mutual data and improve the system's performance. Our simulation results demonstrate that each of the proposed techniques outperformed the one-dimensional (1D) conventional system. Some can provide better bit error rate (BER) performance over the 2D conventional system where the 2D equalizer and 2D soft-output Viterbi algorithm (SOVA) detector are employed to process the obtained readback signals. Furthermore, our findings also indicate that the proposed techniques were robust to media noise. Of the four techniques studied including hard-information flipping (HIF), maximum soft-information (MSI) finding, bit-summation detection (BSD), and multilayer perceptron (MLP), the MLP technique achieved the best performance, at the expense of high complexity.

Author Contributions: Conceptualization, N.R. and C.W.; methodology, N.R., S.K., and C.W.; software, N.R., S.J.G., and C.W.; validation, P.K., S.J.G., and C.W.; formal analysis, S.K., P.K., and C.W.; investigation, S.J.G., and C.W.; writing—original draft preparation, N.R., S.K., P.K., S.J.G., and C.W.; writing—review and editing, N.R. and C.W.; supervision, S.J.G. and C.W.; project administration, C.N.; funding acquisition, N.R. and C.W. All authors have read and agreed to the published version of the manuscript.

Funding: This paper was supported by King Mongkut's Institute of Technology Ladkrabang Doctoral Scholarships (KDS) under Grant KDS2020/012 and King Mongkut's Institute of Technology Ladkrabang Research Fund under Grant number: KREF046705.

Institutional Review Board Statement: Not applicable.

Informed Consent Statement: Not applicable.

Data Availability Statement: Data is contained within the article.

Conflicts of Interest: The authors declare no conflicts of interest.

Appendix *A*

As mentioned earlier, the readback signals from the desired track and two adjacent tracks convey some information about the k-th bit of the l-th track (or the desired track). Therefore, the k-th log-likelihood ratio (LLR) sample produced from the (l-1)-th track, $\{\lambda_{k,l-1}\}$, and the (l+1)-th track, $\{\lambda_{k,l+1}\}$, can be utilized to improve the quality and reliability of the k-th LLR sample from the l-th track, $\lambda_{k,l}$, according to eq. (7) for the bit-summation detection (BSD) technique, which can be proven as follows.

Consider the LLRs of a BPMR channel model in Figure 4. An improved version of the LLR of the k-th bit from the l-th track can be written as

$$\lambda_{k,l}^{\text{new}} = \log\left(\frac{\Pr\left[\lambda_{k,l}=1\middle|\{\boldsymbol{\lambda}\}\right]}{\Pr\left[\lambda_{k,l}=-1\middle|\{\boldsymbol{\lambda}\}\right]}\right), \tag{12}$$

where log(x) is a natural logarithm of x and $\lambda_{k,l}^{\text{new}}$ is the mutual information of $\{\lambda_{k,l-1}\}$, $\{\lambda_{k,l}\}$, and $\{\lambda_{k,l+1}\}$. We have applied the conditional independence relationship in variable form according to [32]

$$\begin{aligned}\Pr\left[A=x\middle|E\right] &= \Pr\left[A=x\middle|B\cap C\cap D\right]\\ &= \Pr\left[A=x\middle|B\right]\cdot\\ &\quad \Pr\left[A=x\middle|C\right]\cdot\Pr(A=x\middle|D),\end{aligned} \tag{13}$$

 doi:10.20944/preprints202501.2382.v1

where A = ∈{±1}, E = x|B ∩ C ∩ D are random variables, and the events B, C, and D are mutually independent. Then, (12) can be expanded to

$$\lambda_{k,l}^{\text{new}} = \log\left(\frac{\Pr\left[u_{k,l}=1\middle|\left\{\lambda_{k,l-1}\right\}\right]\cdot\Pr\left[u_{k,l}=1\middle|\left\{\lambda_{k,l}\right\}\right]\cdot\Pr\left[u_{k,l}=1\middle|\left\{\lambda_{k,l+1}\right\}\right]}{\Pr\left[u_{k,l}=-1\middle|\left\{\lambda_{k,l-1}\right\}\right]\cdot\Pr\left[u_{k,l}=-1\middle|\left\{\lambda_{k,l}\right\}\right]\cdot\Pr\left[u_{k,l}=-1\middle|\left\{\lambda_{k,l+1}\right\}\right]}\right), \tag{14}$$

where {l−1, l, l+1} are the upper track, desired track, and lower track, respectively. Therefore, it can be shown that

$$\Pr\left[u_{k,l}=1\middle|\left\{\lambda_{k,l}\right\}\right]=\frac{e^{\lambda_{k,l}/2}}{e^{\lambda_{k,l}/2}+e^{-\lambda_{k,l}/2}}, \tag{15}$$

and

$$\Pr\left[u_{k,l}=-1\middle|\left\{\lambda_{k,l}\right\}\right]=\frac{e^{-\lambda_{k,l}/2}}{e^{\lambda_{k,l}/2}+e^{-\lambda_{k,l}/2}}. \tag{16}$$

By substituting (15) – (16) into (14), one obtains

$$\lambda_{k,l}^{\text{new}} = \log\left(\frac{\left(\frac{e^{\lambda_{k,l-1}/2}}{e^{\lambda_{k,l-1}/2}+e^{-\lambda_{k,l-1}/2}}\right)\cdot\left(\frac{e^{\lambda_{k,l}/2}}{e^{\lambda_{k,l}/2}+e^{-\lambda_{k,l}/2}}\right)\cdot\left(\frac{e^{\lambda_{k,l+1}/2}}{e^{\lambda_{k,l+1}/2}+e^{-\lambda_{k,l+1}/2}}\right)}{\left(\frac{e^{-\lambda_{k,l-1}/2}}{e^{\lambda_{k,l-1}/2}+e^{-\lambda_{k,l-1}/2}}\right)\cdot\left(\frac{e^{-\lambda_{k,l}/2}}{e^{\lambda_{k,l}/2}+e^{-\lambda_{k,l}/2}}\right)\cdot\left(\frac{e^{-\lambda_{k,l+1}/2}}{e^{\lambda_{k,l+1}/2}+e^{-\lambda_{k,l+1}/2}}\right)}\right), \tag{17}$$

which can be rewritten as

$$\begin{aligned}\lambda_{k,l}^{\text{new}} &= \log\left(\frac{e^{\lambda_{k,l-1}/2}\cdot e^{\lambda_{k,l}/2}\cdot e^{\lambda_{k,l+1}/2}}{e^{-\lambda_{k,l-1}/2}\cdot e^{-\lambda_{k,l}/2}\cdot e^{-\lambda_{k,l+1}/2}}\right),\\ &= \log\left(e^{\lambda_{k,l-1}}\right)+\log\left(e^{\lambda_{k,l}}\right)+\log\left(e^{\lambda_{k,l+1}}\right),\\ &= \lambda_{k,l-1}+\lambda_{k,l}+\lambda_{k,l+1}.\end{aligned} \tag{18}$$

Clearly, (18) is same as (7).

References

1. Wood, R. The feasible of magnetic recording at 1 terabit per square inch. in IEEE Trans. Magn. **2000**, 36, 36-42.
2. Ross, C. Patterned magnetic recording media. Annual Review of Materials Research. **2001**, 31, 203-235.
3. White, R. L.; Newt, R. M. H.; Pease, R. F. W. Patterned media: a viable route to 50 Gbit/in² and up for magnetic recording?. in IEEE Trans. Magn. **1997**, 33, 990-995.
4. Shiroishi, Y.; Fukuda, K.; Tagawa, I.; Iwasaki, H.; Takenoiri, S.; Tanaka, H.; Mutoh, H.; Yoshikawa, N. Future options for HDD storage. in IEEE Trans. Magn. **2009**, 45, 3816-3822.
5. Richter, H. J.; Dobin, A. Y.; Gao, K.; Heinonen, O.; Van de Veerdonk, R. J.; Lynch, R. T.; Xue, J.; Weller, D. K.; Asselin, P.; Erden, M. F.; Brockie, R. M. Recording on bit-patterned media at densities of 1Tb/in² and beyond. 2006 IEEE International Magnetics Conference (INTERMAG), **2006**, 721-721.
6. Wood, R.; Williams, M.; Kavcic, A.; Miles, J. The feasibility of magnetic recording at 10 terabits per square inch on conventional media. in IEEE Trans. Magn. **2009**, 45, 917-923.
7. Nabavi, S.; Kumar, B. V. K. V. Two-dimensional generalized partial response equalizer for bit-patterned media. in 2007 IEEE International Conference on Communications, **2007**, 6249-6254.
8. Nabavi, S. Signal processing for bit-patterned media channel with inter-track interference. Ph.D, Dept. Elect. Eng. Comp. Sci. Carnegie Mellon University, 2008.

 doi:10.20944/preprints202501.2382.v1

9. Nabavi, S.; Vijaya Kumar, B. V. K.; Bain, J. A. Two-dimensional pulse response and media noise modeling for bit-patterned media. in IEEE Trans. Magn. **2008**, 44, 3789-3792.
10. Nutter, P. W.; Ntokas, I. T.; Middleton, B. K. An investigation of the effects of media characteristics on read channel performance for patterned media storage. in IEEE Trans. Magn. **2005**, 41, 4327-4334.
11. Ng, Y.; Cai, K.; Kumar, B. V. K. V.; Chong, T. C.; Zhang, S.; Chen, B. J. Channel modeling and equalizer design for staggered islands bit-patterned media recording. in IEEE Trans. Magn. 2012, 48, 1976-1983.
12. Busyatras, W.; Warisarn, C.; Koonkarnkhai, S.; Kovintavewat, P. A simple 2D modulation code in single-reader two-track reading BPMR systems. Digit. Commun. Netw. **2021**, 7, 100 – 106.
13. Mathew, G.; Hwang, E.; Park, J.; Garfunkel, G.; Hu, D. Capacity advantage of array-reader-based magnetic recording (ARMR) for next-generation hard disk drives. in IEEE Trans. Magn. **2014**, 50, 155-161.
14. Hwang, E.; et al. Performance evaluation of array-reader-based magnetic recording with a drive-tap measurement platform. in IEEE Trans. Magn., **2014**, 50, 1-4.
15. Koonkarnkhai, S.; Kovintavewat, P. An iterative ITI cancellation method for multi-head multi-track bit-patterned magnetic recording systems. Digit. Commun. Netw. **2021**, 7, 107–112.
16. Buajong, C.; Warisarn, C.; Koonkarnkhai, S.; Kovintavewat, P. An intertrack interference (ITI) subtraction scheme for bit-patterned media recording. 2021 18th International Conference on Electrical Engineering/Electronics, Computer, Telecommunications and Information Technology (ECTI-CON), Chiang Mai, Thailand, **2021**, 608-611.
17. Hwang, E.; et al. Skew-dependent performance evaluation of array-reader-based magnetic recording with dual-reader. in IEEE Trans. Magn., **2015**, 51, 1-7.
18. Warisarn, C.; Busyatras, W.; Myint, L. M. M. Soft-information flipping approach in multi-head multi-track BPMR systems. AIP Advances 8, 056509 (**2018**).
19. Busyatras, W.; Warisarn, C. Soft-information flipping scheme based on a priori LLRs summation for ultra-high density magnetic recording. AIP Advances 10, 025217 (**2020**).
20. Shen, J.; Aboutaleb, A.; Sivakumar, K.; Belzer, B. J.; Chan, K. S.; James, A. Deep neural network a posteriori probability detector for two-dimensional magnetic recording. in IEEE Trans. Magn., **2020**, 56, 1-12.
21. Shen, J.; Belzer, B. J.; Sivakumar, K.; Chan, K. S.; James, A. Convolutional neural network based symbol detector for two-dimensional magnetic recording. in IEEE Trans. Magn. **2021**, 57, 1-5.
22. Jeong, S.; Lee, J. Soft-output detector using multi-layer perceptron for bit-patterned media recording. Applied Sciences (2022).
23. Sayyafan, A.; Belzer, B. J.; Sivakumar, K.; Shen, J.; Chan, K. S.; James, A. Deep neural network based media noise predictors for use in high-density magnetic recording turbo-detectors. in IEEE Trans. Magn. **2019**, 55, 1-6.
24. Nguyen, T. A.; Lee, J. Serial detection with neural network-based noise prediction for bit-patterned media recording systems. Applied Sciences 11, **2021**.
25. Rueangnetr, N.; Myint, L. M.; Warisarn, C. Soft-information flipper based on long-short term memory networks for ultra-high density magnetic recording. AIP Advances 11, 015307.
26. Busyatras, V.; et al. Utilization of multiple read heads for TMR prediction and correction in bit-patterned media recording. AIP Advances 7, 056501 (**2017**).
27. Warisarn, C.; et al. Mitigation of TMR using energy ratio and bit-flipping techniques in multitrack multihead BPMR systems. in IEEE Trans. Magn., **2017**, 53.
28. Khankhunthod, K.; Warisarn, C. Track misregistration mitigation using CNN-based method on single-reader/two-track reading BPMR systems. in IEEE Access, **2023**.

 doi:10.20944/preprints202501.2382.v1

29. Yuan, Z. M.; Ong, C. L.; Leong, S. H.; Zhou, T. Liu, B. 3-D sensitivity function of shielded reader by reciprocity principle. in IEEE Trans. Magn. **2010**, 46, 1929-1932.
30. Okamoto, Y.; Ozaki, K.; Yamashita, M.; Nakamura, Y.; Osawa, H.; Muraoka, H. Performance evaluation of ITI canceller using granular medium model. in IEEE Trans. Magn. **2011**, 47, 3570-3573.
31. Karakulak, S.; Siegel, P. H.; Wolf, J. K.; Bertram, H. N. Joint-track equalization and detection for bit patterned media recording. in IEEE Trans. on Magn. **2010**, 46, 3639-3647.
32. Pishro-Nik, H. Introduction to probability, statistics, and random processes. Kappa Research, LLC, **2014**.